

# Electrically and magnetically tunable microwave device using (Ba, Sr) TiO<sub>3</sub>/Y<sub>3</sub>Fe<sub>5</sub>O<sub>12</sub> multilayer

W.J. Kim<sup>1,\*</sup>, W. Chang<sup>2</sup>, S.B. Qadri<sup>2</sup>, H.D. Wu<sup>1</sup>, J.M. Pond<sup>2</sup>, S.W. Kirchoefer<sup>2</sup>, H.S. Newman<sup>2</sup>, D.B. Chrisey<sup>2</sup>, J.S. Horwitz<sup>2</sup>

<sup>1</sup> SFA Inc., 1401 McCormick Dr. Largo, MD 20774

<sup>2</sup> Naval Research Laboratory, 4555 Overlook Ave., Washington D.C. 20375

Received: 3 March 2000/Accepted: 28 March 2000/Published online: 7 June 2000 – © Springer-Verlag 2000

**Abstract.** Ferroelectric (Ba<sub>0.6</sub>Sr<sub>0.4</sub>)TiO<sub>3</sub> (BST) thin films have been deposited by pulsed laser deposition onto single-crystal Y<sub>3</sub>Fe<sub>5</sub>O<sub>12</sub> (YIG) substrates with/without a MgO buffer layer. The structure and microwave properties of the BST films have been investigated as a function of substrate orientation and O<sub>2</sub> deposition pressures (50–800 mTorr). The crystallographic orientation of BST film varies with the deposition conditions. The dielectric properties of the ferroelectric were measured using interdigitated capacitors deposited on top of the BST film. BST films exhibit high tunability (20%–40%) and high dielectric  $Q = 1/\tan \delta$  (30–50) with a dc bias field of 67 kV/cm at 10 GHz. A coplanar waveguide transmission line was fabricated from a (001)-oriented BST film on (111)YIG which exhibited a 17° differential phase shift with an applied dc bias field of 21 kV/cm (10 GHz). An equivalent differential phase shift was achieved with a magnetic field of 160 Gauss.

**PACS:** 81.15.Fg; 84.40. Lj; 77.84.Dy

Electrically tunable ferroelectric thin films are being used to develop a new class of tunable microwave devices [1–8]. The ferroelectric material, (Ba<sub>x</sub>Sr<sub>1-x</sub>)TiO<sub>3</sub> (BST), exhibits a large electric-field-dependent dielectric constant (permittivity), which can be used to produce a resonant frequency shift in a tunable oscillator or a propagation time delay (phase shift) in a transmission line. A concern in the development of tunable microwave circuits is the large change in the characteristic impedance ( $Z_0$ ) of the device, which occurs when the dielectric constant of the ferroelectric is reduced by a factor of four or more with an applied dc bias field. A poor impedance match at the device will increase the reflection and total insertion loss of the device. A novel approach to this problem is to fabricate devices from a ferroelectric/ferrite multilayer to actively adjust the characteristic impedance of the device by changing the dielectric constant of ferroelectric and permeability of ferrite.

In a coplanar waveguide (CPW) transmission line, the differential phase shift ( $\Delta\phi$ ) between two bias states can be

expressed by following:

$$\Delta\phi = \frac{2\pi f}{c} l \left( \sqrt{\varepsilon_{\text{eff}}^1 \mu_{\text{eff}}^1} - \sqrt{\varepsilon_{\text{eff}}^2 \mu_{\text{eff}}^2} \right), \quad (1)$$

where  $f$  is the operating microwave frequency,  $l$  is the length of transmission line,  $c$  is the speed of light in vacuum, and  $\varepsilon_{\text{eff}}$  and  $\mu_{\text{eff}}$  are effective dielectric constant and permeability of device, respectively, and superscript 1 and 2 are for the zero bias and applied bias states, respectively. The characteristic impedance  $Z_0$  of the CPW transmission line is related as:

$$Z_0 \propto \frac{\sqrt{\mu_{\text{eff}}}}{\sqrt{\varepsilon_{\text{eff}}}}. \quad (2)$$

From (1) and (2), it is clear that  $\Delta\phi$  and  $Z_0$  can be engineered by changing  $\varepsilon_{\text{eff}}$  and/or  $\mu_{\text{eff}}$ .

In this paper, we report the growth and characterization of ferroelectric/ferrite multilayers to demonstrate independent control of the characteristics of the transmission line, and to lay the foundation for the development of a constant impedance device. The selected materials for the ferroelectric/ferrite multilayer structure are pulsed laser deposited BST thin films and LPE-grown single-crystal Y<sub>3</sub>Fe<sub>5</sub>O<sub>12</sub> (YIG), respectively. Jia et al. [8] recently reported the growth of BST films on polycrystalline YIG with buffer layers and microwave properties at 100 kHz. BST films show a large dielectric constant change and low loss with dc bias electric field at  $\approx 10$  GHz [1, 5] and YIG shows a large permeability change and low loss with applied magnetic field at  $\approx 10$  GHz [3, 9].

## 1 Experiment

Single-phase (Ba<sub>0.6</sub>Sr<sub>0.4</sub>)TiO<sub>3</sub> (BST) films were deposited using pulsed laser deposition (PLD) onto LPE-grown single-crystal (001) or (111)YIG ( $\approx 100 \mu\text{m}$  thick) on single-crystal Gd<sub>3</sub>Ga<sub>5</sub>O<sub>12</sub>. A short pulse of KrF excimer laser (2480 Å, 30 ns FWHM) was focused on to the rotating BST target with energy density of  $\approx 2 \text{ J/cm}^2$  in flowing O<sub>2</sub> at pressures between 50 and 800 mTorr. PLD provides unique advantages for the deposition of multi-component oxide

\*Corresponding author. (E-mail: kwg@ccf.nrl.navy.mil)

films because it reproduces the stoichiometry of the target in the deposited film [10]. To grow (001)-oriented epitaxial BST films on (001)YIG, a thin layer of MgO has been deposited on YIG prior to the BST deposition. An MgO layer was deposited from a single-crystal MgO target at temperature between 750–850 °C in flowing O<sub>2</sub> at pressure 50 mTorr. The thicknesses of the MgO and BST were  $\approx 1000$  and  $\approx 5000$  Å, respectively. The structure of the multilayer films were measured by X-ray diffraction (XRD) using a Rigaku rotating-anode X-ray diffractometer and a Huber 4-circle X-ray diffractometer using Cu  $K_{\alpha 1}$  radiation. Cross-sectional views of the multilayer films were investigated by a Philips CM-30 transmission electron microscopy (TEM). Microwave properties of the BST films on YIG were measured at 0.1–20 GHz range by an HP 8510C network analyzer using interdigitated capacitors and CPW transmission lines fabricated from depositing Au/Ag by e-beam evaporation through a PMMA lift-off mask [11]. Dielectric constants were extracted using a modified conformal-mapping partial-capacitance method from the measured capacitance and dimensions of the capacitors [12].

## 2 Results and discussion

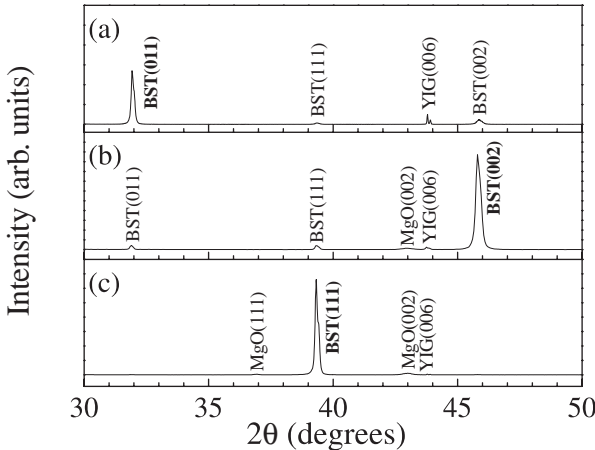
The crystallographic orientation of the deposited BST thin film depends on the crystallographic orientation of the YIG substrate and the deposition conditions. Further, the deposition of a thin layer of MgO prior to the BST deposition can also influence the crystallographic orientation of the BST film. We investigated the BST film growth on (001) and (111)YIG substrates. The substrate temperature for the BST film deposition onto YIG was fixed at 850 °C in order to grow a BST film with a large dielectric constant change with applied dc electric field.

Figure 1 shows XRD patterns obtained for BST films deposited onto (001)YIG substrates with/without a thin MgO buffer layer. Though the lattice mismatch is less than 3% between 3 times of the bulk lattice parameter of BST (3.965 Å) and that of YIG (12.380 Å), the deposited BST film on (001)YIG at 850 °C without an MgO layer is a single phase and polycrystalline with a strong (011)BST reflection

(Fig. 1a). This indicates that the orientation of BST grains in the film are randomly distributed like those in the BST bulk which has the strongest intensity at (011) reflection. It is worth noting that the lattice mismatch between BST and MgO is more than 6%, however, (001)-oriented epitaxial BST films are readily observed on (001)MgO.

To grow an epitaxial BST film on (001)YIG, a 1000-Å-thick MgO buffer layer was deposited prior to the deposition of the BST layer. Figure 1b, c show XRD patterns of BST/MgO/YIG multilayers. The orientation of BST film deposited at 850 °C on MgO/YIG shows a strong dependence on the MgO deposition temperature (750–850 °C). Strong (002) reflections from BST and MgO are observed from BST/MgO layers deposited at 850 °C and 750 °C, respectively (Fig. 1b). The BST/MgO layers deposited at the same temperature (850 °C) exhibit relatively strong (111) reflections of BST and MgO (Fig. 1c). The intensity of the MgO reflections are weak due to the thickness of MgO layers ( $\approx 1000$  Å). The in-plane orientation was investigated by a 4-circle X-ray diffractometer. A BST(850 °C)/MgO(750 °C)/YIG multilayers grows epitaxially;  $\langle 001 \rangle \text{BST} \parallel \langle 001 \rangle \text{MgO} \parallel \langle 001 \rangle \text{YIG}$  with a  $\approx 18.5^\circ$  rotation in in-plane direction between  $\langle 010 \rangle \text{BST} \parallel \langle 010 \rangle \text{MgO}$  and  $\langle 010 \rangle \text{YIG}$ , which is the same as those reported from YBCO/MgO/YIG multilayers [13]. For the BST(850 °C)/MgO(850 °C)/YIG structure, surface normal direction has a very simple relationship ( $\langle 111 \rangle \text{BST} \parallel \langle 111 \rangle \text{MgO} \parallel \langle 001 \rangle \text{YIG}$ ). However, the in-plane orientation of the BST film is a little more complicated;  $\langle 011 \rangle \text{BST}$  directions are parallel with  $\langle 010 \rangle$  or  $\langle 100 \rangle \text{YIG}$  directions, resulting in two BST variants, rotated by 90°. As a result, 12 (024)BST reflections, 6 reflections from each variant, were observed in a 4-circle X-ray diffractometer measurement (Fig. 2). A cross-sectional bright field image of BST/MgO/YIG (Fig. 3) studied by TEM shows columnar grains of BST films with 500–1000 Å column width, which is typical for the films grown by PLD. The column width of BST grains at the interface between BST and MgO is narrower than that at the interface BST and air, which indicates grain growth along in-plane direction during deposition.

Figure 4 shows XRD patterns for BST films grown on (111)YIG single crystals with different O<sub>2</sub> deposition pres-



**Fig. 1a–c.** XRD patterns of BST/MgO/(001)YIG show different orientations of BST: **a** (011)BST/YIG, **b** (001)BST/MgO/YIG, and **c** (111)BST/MgO/YIG

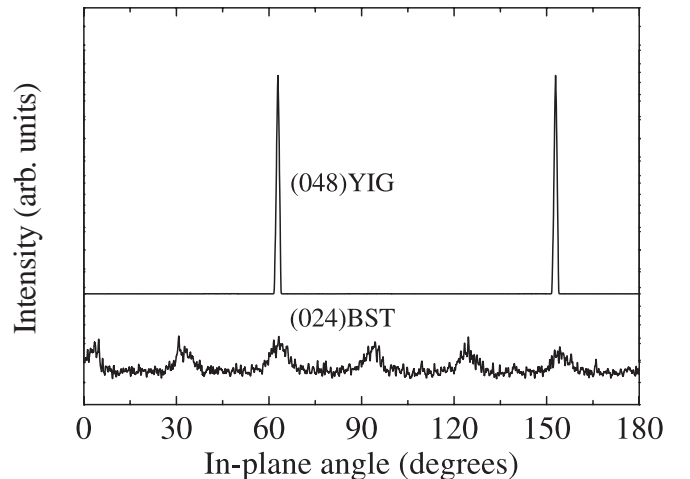


**Fig. 2.** The XRD  $\phi$  scan from (048)YIG and (024)BST reflections

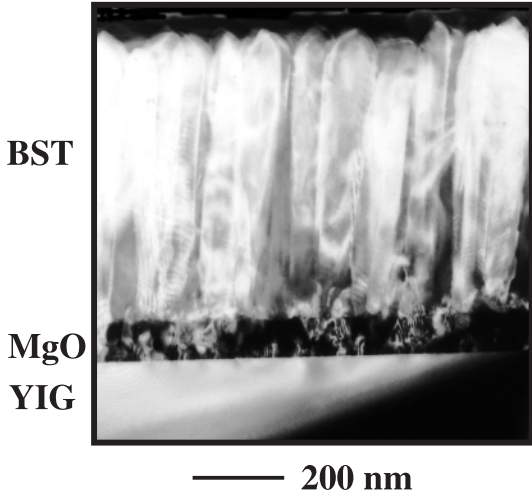


**Fig. 3.** A cross-sectional TEM image of BST(850 °C)/MgO(750 °C)/(001)YIG

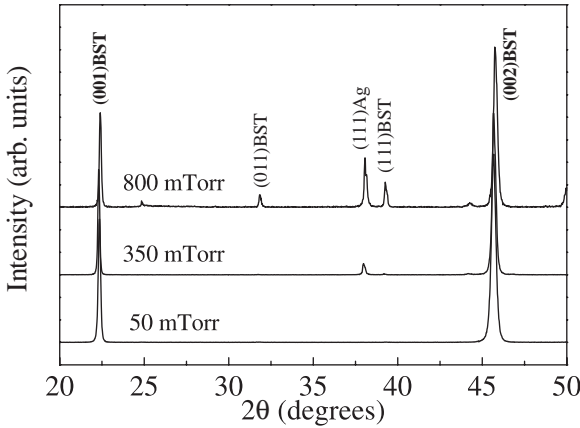


**Fig. 4.** XRD patterns of BST grown on (111)YIG with different O<sub>2</sub> deposition pressures. All BST films show a preferential growth along (001) direction

tures of 50, 350, and 800 mTorr (from bottom to top) at a substrate temperature of 850 °C. An interesting relationship between the structure and microwave properties was previously observed for epitaxial (Ba<sub>0.5</sub>Sr<sub>0.5</sub>)TiO<sub>3</sub> films deposited on MgO using different O<sub>2</sub> deposition pressures [5]. In this study, a large tetragonal distortion was observed in the deposited films. The distortion was a minimum for films grown at 50 mTorr, which also corresponded to films with a high dielectric constant and a large dielectric constant change with applied dc bias field at 10 GHz [5]. All three BST films grown on (111)YIG exhibit intense (001) and (002) reflections, indicating that the films are (001)-oriented, however, no preferential in-plane orientational relationship is observed between BST and YIG. Therefore, the BST films are strongly textured but not epitaxial as in the case of BST on MgO and BST on MgO/(001)YIG. The XRD pattern of the BST film deposited in 800 mTorr exhibits weak intensity for (011) and (111) reflections of the BST film, suggesting that this film is less textured than those deposited in 50 and 350 mTorr.

The measured microwave properties, quality factor  $Q$  ( $=1/\tan\delta$ ), dielectric constant and % tuning ( $=(\epsilon_0 - \epsilon_b)/\epsilon_0 \times 100$ , where  $\epsilon_0$  and  $\epsilon_b$  are dielectric constant at 0 and

67 kV/cm), at 10 GHz are summarized and shown in Figs. 5 and 6 for BST on (001) and (111)YIG substrates, respectively. The dielectric constant of the BST films on MgO/(001)YIG ranges from 400 to 1200 (Fig. 5), which is comparable to those measured for BST films on dielectric substrates, such as MgO and LaAlO<sub>3</sub> at 10 GHz [1, 5]. The dielectric constant at zero bias field and % tuning ( $\approx 1200$  and  $\approx 40\%$ , respectively) is a maximum for polycrystalline BST films (labeled as (011) in Fig. 5) on (001)YIG without a MgO buffer layer, and dielectric  $Q$  ranges from 30 to 40. The (001)-oriented BST film on MgO/YIG shows a high value for  $Q$  ( $\approx 40$  with/without dc bias field) and  $\approx 20\%$  tuning. The BST film with the highest dielectric constant shows the largest dielectric constant change ( $\approx 40\%$ ). The polycrystalline BST film shows a better overall figure of merit ( $= Q(0 \text{ kV/cm}) \times \% \text{ tuning}$ ),  $\approx 1100$ , than either the (001)- or (111)-oriented BST films ( $\approx 750$  and  $\approx 870$ , respectively).

A summary of the measured microwave properties of the BST films on (111)YIG is shown in Fig. 6. The  $Q$  increases with increasing oxygen pressure up to 800 mTorr. However, the dielectric constant and % tuning exhibit a maximum at 350 mTorr. The figure of merit ( $= Q(0 \text{ kV/cm}) \times \% \text{ tuning}$ ), for the BST films is a maximum for films grown in 800 mTorr. Interestingly, BST film grown at 800 mTorr is less textured than films deposited in low oxygen deposition pressures.

To investigate electric and magnetic tunability, CPW transmission lines were fabricated by PMMA lift-off method from metal conductor (Au/Ag) on top of (001)BST film deposited on (111)YIG at 350 mTorr. The differential phase shifts ( $\Delta\phi = \phi(\text{zero bias}) - \phi(\text{bias})$ ) were measured as a function of the static magnetic and electric bias field. The center

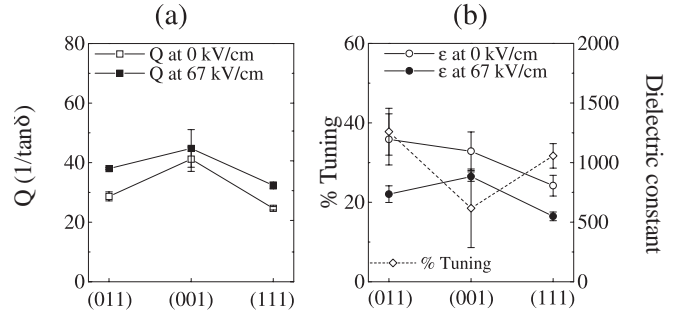


**Fig. 5a,b.** Microwave properties of BST on (001) YIG at 10 GHz: **a** Quality factor  $Q (=1/\tan\delta)$  and **b** dielectric constant and its % tuning

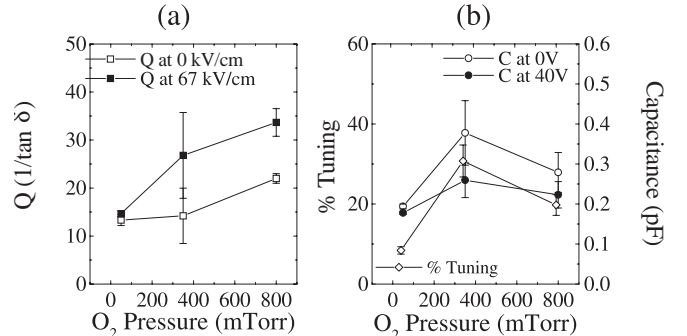


**Fig. 6a,b.** Microwave properties of BST on (111) YIG at 10 GHz: **a** Quality factor  $Q (=1/\tan\delta)$  and **b** dielectric constant and its % tuning

conductor line (1 cm long and 30- $\mu$ m width) is separated by 19  $\mu$ m from ground electrodes as shown in Fig. 7. The dc electric bias field is applied between a center conductor and two ground electrodes, while the magnetic field is applied along a center conductor line. Due to a magnetic resonance between 2.5–3.8 GHz, a complete analysis is difficult. Furthermore, a poor impedance match between probe and CPW, due to an uncertainty of dielectric constant of BST on YIG and limited dimension of CPW mask, leads to a large reflection loss and insertion loss for the CPW structure. A more complete analysis and measurement set-up will be presented in a separate paper [14]. Figure 7 shows the frequency-dependent differential phase shift ( $\Delta\phi$ ) as a function of electric and magnetic bias fields at room temperature. The data presented in the figure are modified without disturbing the nature of frequency dependency of the device. The differential phase shift at 10 GHz is about 17° with a dc electric field of 21 kV/cm. The same amount of differential phase shift at 10 GHz is achieved with magnetic field of 160 Gauss without an electric field. This phase shift is equivalent with  $\approx 4.7$  ps/cm of time delay. With both 21 kV/cm of electric field and 160 Gauss of magnetic field, the measured differential phase shift at 10 GHz is 32° (equivalent to  $\approx 8.9$  ps/cm of time delay). This result (17° and 32° phase shift) is comparable with 12° and 70° for BST films deposited directly onto dielectric substrates (BST/MgO and BST/LaAlO<sub>3</sub>) at 21 kV/cm of electric bias field, though these devices show 90° and 160° phase shift at 10 GHz with 270 kV/cm and 94 kV/cm, respectively [15]. The differential phase shift associated with the electric field increases monotonically with increasing frequency because the dielectric constant of BST is constant at the measured frequency ranges. In contrast, the differential phase shift with magnetic field decreases with increasing frequency. The frequency dependence is consistent with

the differential phase shift calculated by a finite element method [16].

### 3 Summary

In this paper, we report that high-quality single-phase BST films have been deposited onto YIG substrates by PLD. The structure of the BST film on YIG depends on the deposition temperature, buffer layer, and the crystallographic orientation of the YIG. Epitaxial (001) and (111)BST films on (001)YIG were achieved with thin MgO buffer layers. The BST films on (001) and (111)YIG exhibit comparable microwave properties observed from BST films deposited directly onto MgO or LaAlO<sub>3</sub> grown at similar conditions.

Furthermore, we demonstrated electric and magnetic field tuning using a CPW transmission line (1 cm long) fabricated from metal (Au/Ag) conductor on BST film deposited onto (111)YIG. This CPW exhibits a 17° differential phase shift with an applied electric field of 21 kV/cm at 10 GHz at room temperature and an equivalent differential phase shift is achieved with a magnetic field of 160 Gauss applied along the center conductor line.

**Acknowledgements.** The authors would like to thank Dr. D. Webb for a helpful discussion. This work was partially supported by DARPA-FAME program.

### References

1. W. Chang, J.S. Horwitz, A.C. Carter, J.M. Pond, S.W. Kirchoefer, C.M. Gilmore, D.B. Chrisey: *Appl. Phys. Lett.* **74**, 1033 (1999)
2. H.D. Wu, F.S. Barnes: *Integrated Ferroelectrics* **22**, 291 (1998)
3. H. Chang, I. Takeuchi, X.-D. Xiang: *Appl. Phys. Lett.* **74**, 1165 (1999)
4. F.A. Miranda, F.W. Van Keuls, R.R. Romanofsky, G. Subramanyam: *Integrated Ferroelectrics* **22**, 317 (1998)
5. W.J. Kim, W. Chang, S.B. Qadri, J.M. Pond, S.W. Kirchoefer, D.B. Chrisey, J.S. Horwitz: *Appl. Phys. Lett.* **76**, 1185 (2000)
6. J. Im, O. Auciello, P.K. Baumann, S.K. Steiffer, D.Y. Kaufman, A.R. Krauss: *Appl. Phys. Lett.* **76**, 625 (2000)
7. A. Kozyrev, A. Ivanov, V. Keis, M. Khazov, V. Osadchy, T. Samoilova, O. Soldatenkov, A. Pavlov, G. Koepf, C. Mueller, D. Galt, T. Rivkin: *IEEE MTT-S* **2**, 985 (1998)
8. Q.X. Jia, J.R. Groves, P. Arendt, Y. Fan, A.T. Findikoglu, S.R. Foltyn, H. Jiang, F.A. Miranda: *Appl. Phys. Lett.* **74**, 1564 (1999)
9. D.E. Otaes, G.F. Dionne, D.H. Temme, J.A. Weiss: *IEEE Trans. Appl. Super.* **7**, 2347 (1997)
10. D.B. Chrisey, G.K. Hubler (Eds.): *Pulsed Laser Deposition of Thin Films* (Wiley, New York 1994)
11. S.W. Kirchoefer, J.M. Pond, A.C. Carter, W. Chang, K.K. Agarwal, J.S. Horwitz, D.B. Chrisey: *Microwave Opt. Technol. Lett.* **18**, 168 (1997)
12. S.S. Gevorgian, T. Martinsson, P.I.J. Linner, E.L. Kollberg: *IEEE Trans. Microwave Theory Tech.* **44**, 896 (1996)
13. A. Pique: Ph.D. Thesis, Univ. of Maryland (1996)
14. S.W. Kirchoefer, J.M. Pond, H.S. Newman, W.J. Kim, J.S. Horwitz: *IEEE MTT*, to be published
15. J.M. Pond, S.W. Kirchoefer, W.J. Kim, W. Chang, J.S. Horwitz: *IEEE MTT*, to be published
16. L. Zhou, L.E. Davis: *IEE Proc. Microwave Antennas Propagation* **144**, 111 (1997)

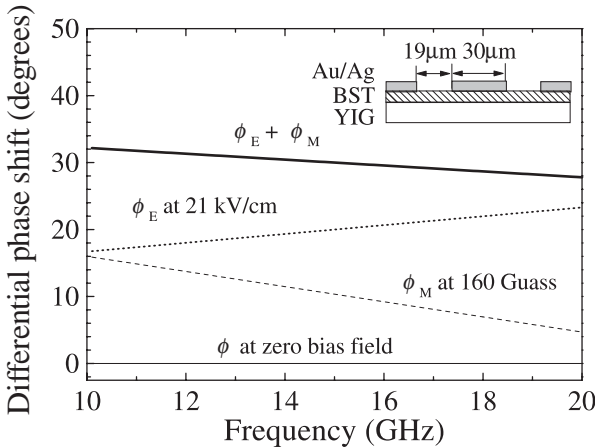


**Fig. 7.** Measured differential phase shift ( $\Delta\phi = \phi(\text{no bias}) - \phi(\text{bias})$ ) from CPW transmission lines fabricated on ferroelectric BST films grown on ferrite (111)YIG with electric dc bias field of 21 kV/cm and/or magnetic field of 160 Gauss